Bulletin of the Geological Survey of Japan, Vol. 47 (11), p. 577-597, 1996

Genetic model of gold-antimony-tungsten mineralization: evidence from geology and mineralization of the Wuxi deposit, Hunan, China

Xiongwei HU*, Satoshi MURAO** and Xuchang HUANG***

HU Xiongwei, MURAO Satoshi and HUANG Xuchang (1996) Genetic model of gold-antimony-tungsten mineralization: evidence from geology and mineralization of the Wuxi deposit, Hunan, China. *Bull. Geol. Surv. Japan*, vol. 47(11), p. 577-597, 12figs., 3 tables.

Abstract: The Wuxi deposit, situated in the Xuefeng arctuate uplifted belt, western Hunan, China, is a representative of composite gold, antimony and tungsten deposits in China. The mineralization is of bedding-parallel vein type hosted by Upper Proterozoic calcareous sericitic slates and controlled by interlayer faults and north-east trending secondary folds. Strike of ore veins is approximately 6km with extensions of more than 1km with significant Au, Sb and W content. The average ore grade at Wuxi is 8.38ppm Au, 4.36wt.% Sb and 0.37 wt.% WO_3.

The mineralization at the Wuxi deposit took place during the Mesozoic Era under the framework of detachment structures and is closely associated with the formation of composite quartz veins in which seven phases showing temporal differences are distinguished. The mineralization can be divided into two stages of tungsten mineralization (stage I) and gold-antimony mineralization (stage II). The tungsten mineralization is comprised of scheelite substage (Ia) and wolframite substage (Ib) corresponding to two vein phases. The gold-antimony mineralization is composed of a pyrite-quartz vein phase and a stibnite-quartz vein phase both of similar origin but distinct from tungsten mineralization. Scheelite deposition most likely resulted from acidic solutions that underwent neutralization, whereas ferberite precipitation resulted from acidation of solutions. Gold and antimony might be co-transported in weakly alkaline fluids and precipitated by cooling and acidation of fluids. The deposit can be categorized as a spatially coupled tungsten mineralization and gold-antimony mineralization.

Our re-examination supports a genetic model for the origin of ore-forming fluids from deep convection and chemically evolved paleo-ground water. We propose that fluid discharging from a deep system into the shallow system is a possible mechanism of mineralization. Such a process may be initiated and promoted by formation of brittle faults which serve as the main conduits for upward migration of hydrothermal fluid. Periodic structural mobilization of Mesozoic age is a significant factor controlling composite quartz vein and composite mineralization.

1. Introduction

The Wuxi deposit is a representative composite Au-Sb-W type mineralization in China (Hu *et al.*, 1996). Similar deposits, such as Au-Sb or W-Sb mineralization, are wide-

*(STA Fellow in 1996, Mineral Resources Department, GSJ)
Yichang Institute of Geology and Mineral Resources, Chinese Academy of Geological Sciences.
**(Mineral Resources Department, GSJ)
***(Geological Division, Xiangxi Gold Mine, Hunan, China.)

Keywords : gold, antimony, tungsten, Wuxi (Woxi) deposit, composite deposit, spatially-coupled deposit, China.

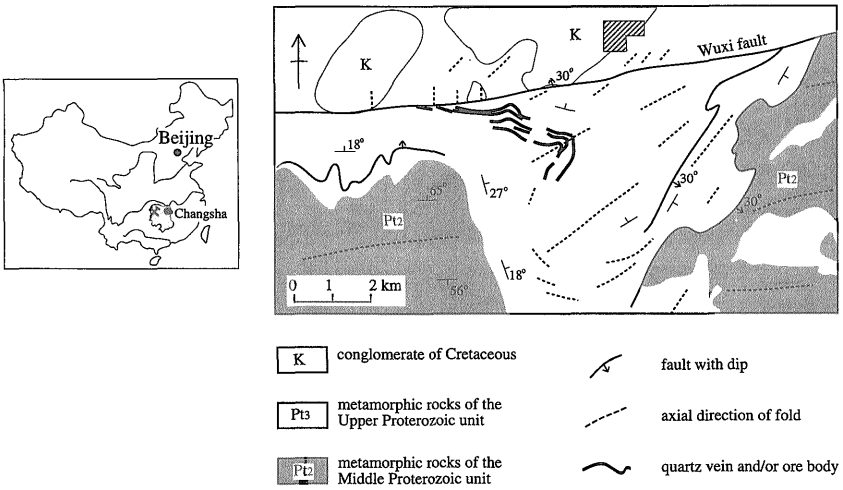

Fig. 1 Geological map of the Wuxi gold-antimony-tungsten deposit, Hunan, China (simplified after Luo *et al.*, 1984). Note diffrent structural features in various tectonic layers. Interlayer detachment faults and northeast trending folds are limited to the Banxi Group of the Upper Proterozoic unit.

spread in Hunan, China, and also in other countries, e.g. Bolivia, Spain, Germany, France and Turkey (Dill *et al.*, 1995; Gumiel and Arribas, 1987). The gold-antimony deposit is an important antimony producer in Bolivia (Dill *et al.*, 1995). Being different from other gold-antimony or gold-antimony -tungsten deposits where it is difficult to recover gold, (e.g., Kharma deposit in Bolivia: Dill *et al.*, 1995), the Wuxi deposit is characterized by economic grades of gold, antimony and tungsten. At the Wuxi deposit, gold has been mined since 1875, while antimony ore was found in 1889 and tungsten in 1946. Antimony and tungsten were the main products during the 1950's and 1960's. At present, the Wuxi mine is a major gold producer of Hunan Province, China, where antimony and tungsten are also produced.

The Wuxi deposit is located about 200km west of Changsha, the capital of the Hunan Province, China (Fig. 1). The deposit is tectonically situated in the Xuefeng arcuate uplifted belt which is a significant Au, Sb and W mineralized belt in which many Au, Au-Sb, W-Sb, Au-Sb-W deposits occur. The Wuxi is the northwesternmost deposit in the belt, where the north-northeast strike bends to east -west. Within the belt other representatives are Xichong Au-Sb, Zhazixi W-Sb, Fuzhuxi Au-Sb, Mobin Au and Xi'an W deposits, etc. (Li, 1987).

During the past decade, the Wuxi deposit (also refereed as to Woxi) has been geologically described (Hunan Metallurgic Geological Party No. 237, 1978, unpublished paper; Li, 1989) and genetically discussed with respect to tungsten, gold mineralization and antimony mineralization (Liu *et al*, 1983; Bao, 1988; Wu *et al.*, 1989; Shi *et al.*, 1993). Mineralogical work on ore, geochemical studies of alteration and fluid inclusions as well as sulfur, oxygen, and hydrogen isotopic studies have been done since 1984 (Luo *et al.*, 1984; Bao and He, 1991; Wang, 1993; Zhang, 1985; Liang and Zhang, 1986). Three kinds of genetic models have arisen from these earlier studies: 1) Epithermal deposit originating from magmatic fluid (Hunan Metallurgical Geological Party No. 237, 1978, an unpublished paper; Yang, 1986). Yang proposed that mineralization might take place during the Later Yanshanian acidic magmatism. 2) Sedimentary-metamorphic models. These consist of a number of widely accepted hypotheses which assume metamorphic solutions are the main component of ore

forming fluids (Liu *et al.*, 1983; Luo *et al.*, 1984). However, no conclusive model has been proposed because of divergences on the ore forming process. Sedimentation and/or metamorphism are considered to be significant in the ore forming process. Therefore, the deposit is referred to as either sedimentary -metamorphosed or sedimentary-metamorphic deposit and metamorphic deposit (Xiao and Li, 1984; Zhang, 1985; Bao, 1988; Li, 1989; Bao and He, 1991). 3) Hydrothermal model for fluid originating from circulating paleo -ground-water (Shi *et al.*, 1993; Shi and Hu, 1994) which proposed that antimony mineralization took place within a "paleo-hydrothermal field" during the Mesozoic Era.

The principle objectives of this paper are to re-examine the geology and mineralization of the Wuxi deposit on the basis of field and microscopic observations of ores as well as careful review of previous data, to discuss relationships of gold, antimony and tungsten mineralization and to develop a comprehensive geologic-genetic model for the deposit.

The specimens in this report were taken from representative ore bodies of the deposit, No. 3 and No. 4 veins, veinlets and ceiling or floor veins of the No. 3 vein. Three galleries were sampled (150m level above sea level, -185m level below sea level and -210m level). Underground examinations were also taken on No. 1 and No. 3 veins at the -60m level gallery.

2. Geological setting

The Xuefeng arcuate tectonic belt, tectonically being a part of Jiangnan Uplift of Yangzi Platform, Southern China, is an anticlinorium consisting of Middle to Upper Proterozoic metamorphic rocks (Lenjiaxi group and Banxi group) mainly, Upper Proterozoic to Lower Paleozoic marine detrital and carbonate rocks and Mesozoic continental clastic rocks locally. The pre-Sinian rocks were deposited in an active synclinal environment characterized by volcano-sedimentary formation and were subsequently metamorphosed to subgreenschist facies and deformed during Xuefengian orogenesis (later Proterozoic in age). The Sinian and Lower Paleozoic sediments formed in a platform environment and were deformed during the Caledonian period (earlier Paleozoic) (Hunan Bureau of Geology and Mineral Resources, 1988). This belt was uplifted after the Ordovician Period and underwent strong structural deformation during the Indosinian and Yanshanian periods (Mesozoic) which were characterized by block faulting and thrusting and are responsible for the development of Mesozoic continental basins.

Composite interlayer-slip structures are a significant tectonic feature of the Xuefeng belt. Sun *et al.* (1993) proposed that there are several kinds of interlayer-slip and/or dipping -sliding structure systems within the Banxi Group characterized by four-D deformation, i. e., decoupling-, detachment-, disharmonic - and décollement-structures. It was revealed that development of regional fractures followed a sequence of interlayer-sliding faults through cross-cutting sliding faults to overthrust faults, and finally to nappe structures. In the eastern part of Xuefeng belt, overthrust structures and/or nappe structures have been examined in the Upper Proterozoic unit and timing of structural development to Jurassic or Cretaceous periods is indicated by Proterozoic rocks that structurally overly Mesozoic sediments of Jurassic and/or Cretaceous age (Liu, 1992). Interlayer-slip structures in the Xuefeng belt formed during the Mesozic Era served as the tectonic framework for the mineralization in the study area.

3. Local Geology and mineralization at the Wuxi Deposit

The mining area is composed of Proterozoic metamorphic rocks and Cretaceous continental conglomerate (red sediments) (Fig. 1). The country rock is thick purplishred sericitic slate of the Upper Proterozoic unit with a wide distribution (Madiyi Formation of Banxi Group). The Cretaceous red sediments occur to the north of the EW trending Wuxi fault and are limited to Cretaceous basins. The Wuxi

fault dips towards north at an angle of 30° and cuts the country rocks at a low angle (Fig. 2). There are two other faults occurring in the eastern part of the district with dip directions concordant with strata (Fig. 2) and both these and the Wuxi fault are interlayer faults. The Wuxi fault was considered to be a reverse fault (Li, 1989; Liu, 1993), a positive fault (Shi *et al.*, 1993) and/or a strike-slip fault (Peng, 1991). The fracture zone of the Wuxi fault is 20 to 100 meters wide (Liu, 1993) and several structure planes can be identified within the fracture zone comprised of fault gouge, granulated slate, mylonite, and breccia which indicate a long lived-history. At least, two stages of fault activity with different rheological behaviors can be distinguished, ductile fracture stage and brittle fracture stage. The ductile stage may be earlier than the brittle stage and represents a dip-slip fault movement while the brittle stage may be associated with strike-slip movement. The dextral strike-slip nature of the Wuxi fault is clearly indicated by the occurrence of a set of small northeast striking folds adjacent to the fault which formed by fault drag.

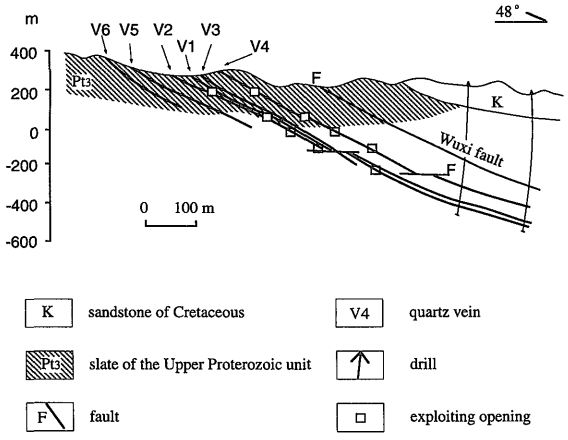

Fig. 2 No. 4 geological section of the Wuxi deposit, Hunan, China, showing the bedding-parallel quartz veins occurring in interlayer faults associated with the Wuxi fault.

The ore controlling structure in the area is interlayer faults/detachment faults contacting the Wuxi at a low angle. Six faults are indicated by the filling of quartz veins (Figs. 1 and 2). These faults belong to secondary faults of the Wuxi fault and are gently dipping and generally concordant with the horizontal bedding of slate.

In the Wuxi district, the Middle Proterozoic unit appears as E-W trending folds, and the Upper Proterozoic unit shows a "sigmoidal type" deformation which resulted from overprinting of northeast trending folds on the E-W trending folds. The northeast trending folds are obviously limited to the Upper Proterozoic unit and are apparently related to the detachment faults including both the Wuxi fault and eastern faults in the district (Fig. 1). Small sliding faults adjacent to quartz veins

Table 1 Timing constraints on geological evolution at the Wuxi deposit, China

Type	Constraint	Evidence
E-W folds	The oldest structure in the mining area	In metamorphic rocks
	Predate or synchronous with the Caledonian period	Concordant with the regional structure line of basement rocks
Wuxi fault	Predates the Cretaceous, postdates the metamorphism which took place during Xuefengian period (Later Proterozoic)	Does not cut through the Cretaceous basin, cuts the metamorphic rocks
Other reverse faults	Postdate the E-W fold and postdate or synchronous with the Wuxi fault	Cut E-W folding direction, does not cut the Wuxi fault
		Limited within Upper Proterozoic Unit
N-E folds	Postdate E-W fold	Overprint on the E-W folds
	Synchronous with the Wuxi fault	Limited to within the Upper Proterozoic Unit
Quartz veins	Postdate or synchronous with the Wuxi fault	Occur in the foot wall of the Wuxi fault and filled along interlayer faults associated the Wuxi fault
	Postdate or synchronous with the NE folding	The quartz veins were deformed and appear in NE-trending folds
	Formed during the Jurassic Period	Rb-Sr isochron age is 144.8±12 Ma*
	Multiple stages of formation	Composite vein in which seven phases can be distinguished
N-S folds	Postdate the Cretaceous period	Occur both in Cretaceous and Upper Proterozoic units of the hanging wall of the Wuxi fault

* Shi et al., 1993

and small sliding folds including folded thin veins (pre-ore phase) can also be examined underground. The Cretaceous strata appears within small NS-trending folds.

The timing of events within the geological evolution of the Wuxi district are shown in Table 1. In spite of the long geological evolution from middle Mesozoic to Cenozoic Era, the Mesozoic Era is specifically emphasized because ore-controlling faults formed in the Jurassic period as indicated by Rb-Sr dating of quartz samples from ores (Shi *et al.*, 1993). Although it is not clear when the Wuxi fault was initiated, spatial relations within the Cretaceous basin implies that the Mesozoic Era is the significant active period of the Wuxi fault. Two stages of the Wuxi fault may correspond to regional tectonic background of foreland nappe structure environment in the Indosinian (Triassic period) and interior extension environment during the Yanshanian period (from Jurassic to Cretaceous in age) (Sun *et al*, 1991).

Quartz veins at the Wuxi deposit structurally occur in interlayer faults and are bedding-parallel and concordant with host slates. Six quartz veins with variable extension of 100m to 5300m have been found at the surface and more concealed quartz veins were revealed during underground exploitation. These veins are sub-parallel to each other with a spacing of 5-80m. Thus, they are also termed "bedded veins" by local geologists.

The bedding-parallel veins at Wuxi are a kind of composite vein system with a mean thickness of 0.4 to 1.4m comprising several vein phases. Seven phases can be distinguished in the composite quartz veins based on recognition of structural features, temporal-spatial relationships, vein fabric, mineral associations and mineralizing character (Table 2). The pre-ore phase (phase 1) and post-ore phase (phase 7) are characterized by transparety quartz which is different from milky or light gray quartz from vein phases 2 to 4. Quartz from vein phases 5 and 6 is characterized by transparent euhedral crystals. The post-ore phase is also characterized by the occurrence of aragonite (Luo *et al.*, 1984). Later vein phases often overprint earlier ones. The main vein phase (phase 4) erased most of previous phases and was overprinted by later

Table 2 Schematic table showing various phases of composite quartz vein through time, Wuxi deposit, Hunan, China

	vein phase	time	mineralization	Evidence
1	pre-ore quartz carbonate vein	early	none	Calcite-quartz vein with small sliding folds.
2	scheelite-bearing quartz vein		W	Scheelite occurs as relicts in quartz vein and cut by later phases.
3	wolframite-bearing quartz vein		W	Occurs as wolframite quartz veins and fissure filling of wolframite crystals.
4	main quartz vein phase		?	Host lithology of gold and antimony mineralization.
5	pyrite (-quartz?) vein		Au	Banded ore formed by pyrite (-quartz) filling fissures in veins.
6	stibnite-quartz vein		Au-Sb	Stibnite fills in fissures of quartz veins showing banded structure or ponded ores.
7	post-ore quartz-carbonate vein	later	none	Calcite-aragonite-quartz vein.

Table 3 A summary of ore bodies at the Wuxi deposit (simplified after Wu et al, 1989 and an unpublished exploration report, 1978)

vein No.	length of vein/alteration (m)	economic ore body numbers	striking (m)	dipping (m)	thickness (m)	average grade Au ppm	Sb (wt.%)	W (wt.%)
1	5300	13	100-320	180-2010	1.35	5.67	1.34	0.22
2	650	2	40-70	360-720	0.42	6.41	4.26	0.55
3	1500	6	30-290	550-1975	0.79	10.33	3.91	0.24
4	100	4	50-350	500-2280	1.01	10.13	5.55	0.76

phases characterized by fissure filling of sulfides in quartz veins. Among the seven phases, only four phases are found to be responsible for mineralization corresponding to tungsten and gold-antimony mineralization. The occurrence of multiple phases implies that the formation of quartz veins is closely related to periodic structural dilations.

Economic orebodies have been found in four quartz veins. Table 3 gives a summary of economic orebodies. No. 1 vein has the longest interrupted exposure of 5300m at the surface and No. 4 vein only exhibits an approximately 100m long alteration zone/belt at the surface. However, the No. 4 vein is the leading vein of the deposit. The economic ore bodies usually appear as bedded column shapes which are about 50 to 350m long in strike, 0.1 to 3m thick and 300 to 1700m long in dip, and are strongly structurally controlled. Such bedded ore bodies occur in the axial parts of northeast-trending anticlines or synclines. Twenty three economic portions have been discovered within the four mineralized quartz veins. Along the strike of interlayer faults, lenticular orebodies and alteration zones are observed alternatively.

Three kinds of ores can be distinguished at the Wuxi deposit. The first is so called "bedded vein ore" which is mineralized interlayer quartz vein concordant with the host strata and is predominant in the mine. The average grade is 8.38ppm Au, 4.36 wt.% Sb and 0.37 wt.% WO_3. The second is veinlet and/or joint vein ore which is composed of a set of high angle (68-70°) thread veins adjacent to the bedded vein. The veinlet usually is 1-4cm thick and 20-30m long (Wang and Yang, 1990). The grade of veinlet ore varies from 0.03 to 2.43wt.% W and from 0.67 to 15.0ppm Au. No antimony mineralization has been reported in the veinlet ore. The third is stockwork ore which is associated with the main vein and shows variable ore body shapes including bed, lenticle, wedge, and pod. The mean grade is 4ppm Au, 1wt.% Sb and 0.16 wt.% W. The veinlet and stockwork ores were considered to be synchronous and have the same genesis with the bedded vein type ores (Huang and Cheng, pers. commun.). It is proposed that the development of bedded veins could be closely related to the development of interformational detachments and veinlets as well as veinlets may be related to interlayer shear.

The ore is composed of native gold, scheelite, stibnite, pyrite, wolframite mainly, with subordinate arsenopyrite, sphalerite, galena and chalcopyrite. Quartz is predominant as a gangue mineral but calcite, ferroandolomite, chlorite, illite, pyrophyllite, and kaolinite are also present. The signature alteration of the deposit is decolourization of purplish-red slate into gray yellow or light yellow slate in which pyritization, muscovitization, sericitic alteration, and silicification can be observed. Chloritization appears as chlorite veinlets in slates which forecasts thinning out of ore bodies. Alteration zoning from quartz veins adjacent to the ore body to those distant from the ore and barren systematically progresses from the muscovite-pyrite zone through the silicification and sericitic altertion zones to sericitic and/or chloritization zones and finally to fresh slate in which iron or titanium oxides remains (Shao *et al.*, 1989).

4. Relationships of tungsten, gold and antimony mineralization

Figure 3 is a geological sketch of quartz vein No. 1 showing the typical banding texture of a composite quartz vein consisting of scheelite relicts enveloped in quartz, pyrite bands filling horizontal fissures in the vein and stibnite bands occurring at the margin of the quartz vein. Phases 2, 4, 5 and 6 can be observed in Figure 3. Mineralization at Wuxi deposit is spatially composite and temporally separated. Here we describe tungsten, gold and antimony mineralization respectively on field evidence and mineral paragenesis.

4.1 Tungsten mineralization

The tungsten mineralization at the Wuxi deposit comprises two phases; scheelite quartz veins and wolframite quartz veins and both are mainly concentrated in the shallow part of the deposit with ore grade decreasing downwards.

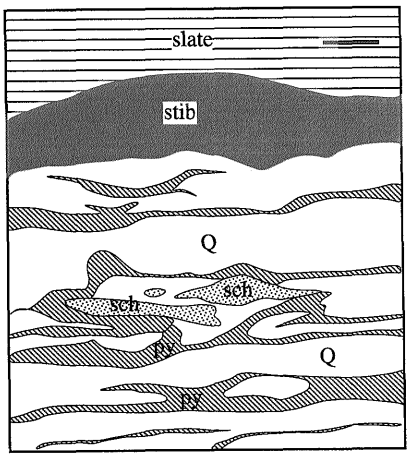

Fig. 3 Underground geologic sketch showing banding texture of composite quartz vein consisting of scheelite relicts (sch, phase 2), main quartz vein phase (Q, phase 4), pyrite-bands (py, phase 5) and stibnite-bands (stib, phase 6) (No. 1 vein, -60m level, western gallery, scale bar=1cm).

Along the strike of the quartz vein from east to west, scheelite concentration decreases and wolframite increases.

The scheelite mineralization (phase 2) is obviously earlier than the wolframite-bearing quartz veins (vein phase 3). Details of the mineral assemblage of the scheelite-quartz phase is not assessable because scheelite generally occurs as relict islands within the veins. Coarse grained scheelite appears white and several centimeters in size exhibiting brecciated or rounded shapes (Figs. 3 and 4a). Scheelite grains are enveloped in quartz aggregate with later fissure filling of wolframite (Figs. 4a and 4b), or cut by pyrite veins (Fig. 4b) and overprinted by stibnite mineralization (Fig. 5). Corroded scheelite is included in quartz with fissure filling of stibnite (Fig. 6 a) or is cemented by stibnite (Fig. 6b). The scheelite quartz vein phase may represent the earliest mineralization at the Wuxi deposit.

Wolframite mineralization is well recorded by wolframite-bearing quartz veins (phase 3) occurring in both composite veins (Fig. 4c)

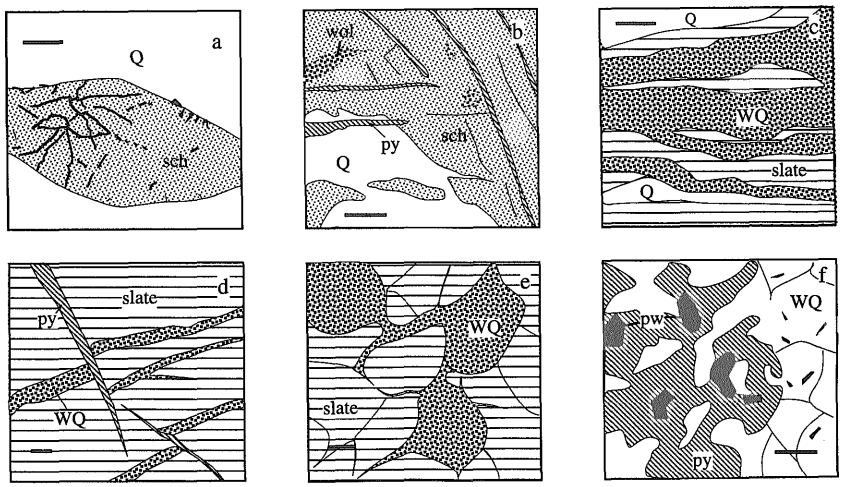

Fig. 4 Sketches of the tungsten mineralization at the Wuxi deposit (scale bar=1 cm). a, tiny wolframite crystals (black) filled in fissures of a scheelite grain (sch) included in quartz (Q) (No. 1 vein, 60m level); b, disseminated wolframite crystals (wol) in scheelite grain (sch) replaced by quartz (Q) and cut by pyrite veins (py) (No. 1 vein, No. 9 steep draft of 60m level); d, wolframite-bearing quartz veins (Wq, phase 3) in slate cut by pyrite veins (py, phase 5) (WQ) in brecciated slate (No. 3 vein, -60m level); f, plate (pw, 4-8mm), needle (0.5-3mm) wolframite crystals and disseminated pyrite in quartz vein (Q) (No. 3 vein, west gallery of -60m level).

and host rocks (Fig. 4d). Wolframite ore nests can be found in brecciated slate (Fig. 4 e). Wolframite quartz veins are later than the scheelite phase (Fig. 4b) and earlier than the formation of pyrite veins (Figs. 4b, 4d). Two generations of wolframite are indicated by two kinds of wolframite crystals, plate-shaped and needle-shaped, in the No. 3 vein (Fig. 4f).

Wolframite at the Wuxi deposit is nearly pure ferberite with MnO/FeO ratio of 0.05 and total $Nb_2O_5+Ta_2O_5$ content of 0.18wt.% (Luo *et al.*, 1984)). This composition is quite different from the wolframite from the Dajishan Mine, Jiangxi, that has MnO/FeO ratio ranging from 1.2 to 3.2, total $Nb_2O_55+Ta_2O_5$ content ranging from 0.47 to 1.37wt.%, and which likely originated from magmatic hydrothermal solution (Shi and Hu, 1988).

4.2 Antimony mineralization

Stibnite is the only primary antimony mineral at the Wuxi deposit, which differs from the Kharma gold-antimony deposit where aurostibnite and Au-Sb oxides were reported (Dill *et al*, 1995). Antimony mineralization at the Wuxi deposit is marked by the formation of stibnite banding in composite quartz veins (Fig. 7a) and veinlet ore in slate (Fig. 7b). Massive stibnite ore pods are not uncommon in composite quartz veins. Banded ore formed by stibnite filling in bedding fractures of quartz veins and massive ore/ore pods formed by open-space filling by stibnite in brecciated quartz veins suggests that brittle deformation occurred after formation of the main quartz veins and was possibly associated with antimony mineralization. Antimony mineralization is apparently later than the formation of the main quartz vein (phase 4). Quartz that is paragenetic with stibnite forms small euhedral crystals included in stibnite crystals or occurs as micro-veins which cut previous phase quartz and scheelite (Fig. 5). It is thus proposed that antimony mineralization at the Wuxi is strongly controlled by fractures or brecciation of quartz veins and is best characterized as a fracture filling type mineraliza-

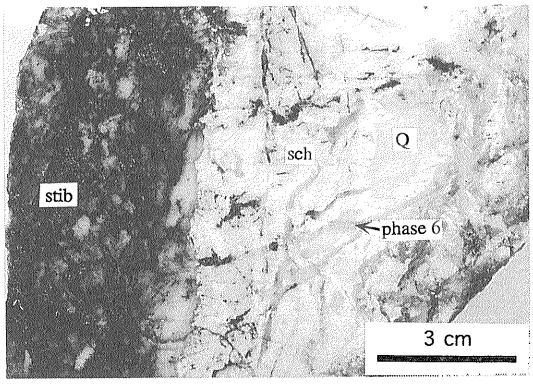

Fig. 5 Photograph of handspecimen showing texture of composite ore from the Wuxi deposit. Note antimony mineralization shows banding in the vein and scheelite is cut by stibnite-quartz veinnet. There are two quartz phases: one is main vein quartz (phase 4) which replaced scheelite (phase 2) and appears as residua in stibnite band; the second is quartz veinnet (phase 6) associated with stibnite which cuts both scheelite and main vein quartz (phase 4).

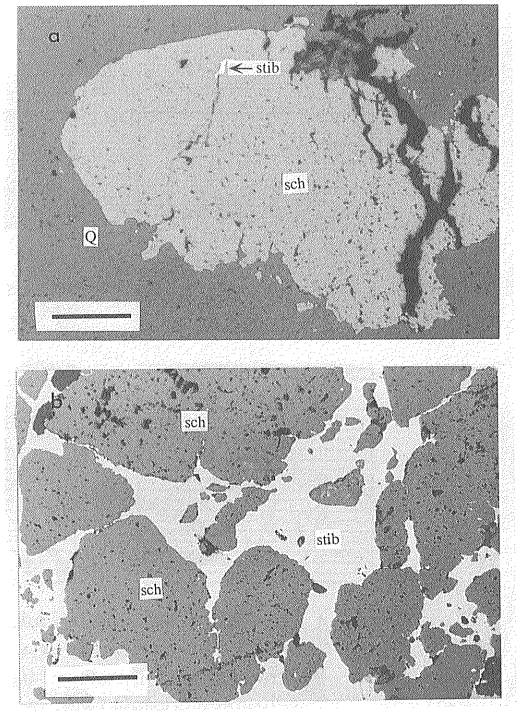

Fig. 6 Photomicrographs showing etched scheelite (sch) in quartz aggregation (Q) (a) and cemented by stibnite (stib) (b). Scale bar=100 micrometer, reflected light.

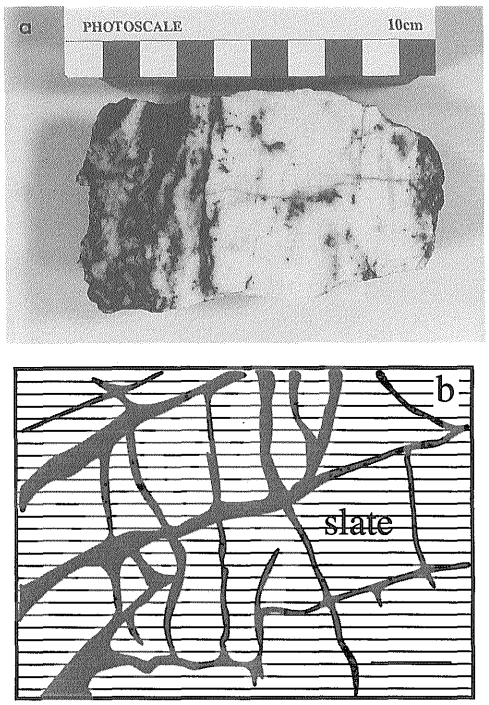

Fig. 7 a, Photograph showing banded stibnite ore formed by stibnite (black) (phase 6) filling in fissured quartz (white) vein (phase 4); b, Stibnite veinlet filling in fissures of slate (adjacent No. 3 vein, west gallery of -60m level).

tion.

4.3 Gold mineralization

Native gold is the only gold mineral at the Wuxi deposit with pyrite and stibnite serving as the main host minerals of gold (Li, 1989; Bao and He, 1991). Native gold grains in our specimens range from 1 to 300 micrometers. Several kinds of gold occurrence are distinguished on the basis of relations with its host mineral. Such occurrence records parts of the history of gold precipitation. Native gold occurrences are summarized as follows.

(1) Gold grains disseminated in quartz aggregates: such gold grains are small with irregular shapes, usually 1-5 micrometers. The gold may be synchronous or postdate the precipitation of quartz (Fig. 8a).

(2) Gold grains closely related to pyrite: three types of pyrite can be distinguished. The first is coarse cubic pyrite showing apparent etch pits. The second is fine cubic and octahedral pyrite showing banded distribution in quartz veins. Both can occur within one specimen from quartz veins. However, the fine grained pyrite is obviously later than coarse grained pyrite. The formation of fine pyrite may result from hydrothermal solution filling because both banded pyrite filled fissures in quartz veins (phase 5) and pure pyrite veins/veinlet in slate are present (Figs. 9a, 9b). The former formed by the overprinting of pyrite-quartz phase on brecciated or fissured quartz veins and the latter formed by pyrite filling in brecciated or fissured slate. Pyrite veins which cut wolframite-bearing quartz veins indicate that they postdate the tungsten mineralization.

Gold grains show close relations with both coarse and fine pyrites. In the case of coarse pyrite, gold grains fill in etch pits of pyrite and/or are enveloped by stibnite (Figs. 8c and 8e), which indicates that gold postdates the pyrite and predates or is synchronous with stibnite. Within fine pyrite bands of the quartz vein, fine irregular gold grains (less than 5 micrometers) are found to be paragenetic with pyrite. In this case, gold apparently precipitated from hydrothermal solution synchronously with the pyrite (Fig. 8d).

The third type of pyrite is paragenetic with stibnite. We observe that gold precipitated on the surface of pyrite (Fig. 8f) and both gold and pyrite are included in stibnite crystals, which indicates that gold postdates the pyrite. Therefore, gold mineralization related to pyrite at the Wuxi deposit is mainly associated with fine grained pyrite which may be a hydrothermal product and later than the main quartz vein phase. Coarse pyrite serves as an important gold host mineral but gold precipitation is later than formation of the pyrite.

(3) Gold grains associated with stibnite: stibnite is another significant gold-bearing mineral in which native gold occurs. Three kinds of gold occurrences can be distinguished on the basis of relations with stibnite: pre-stibnite, syn-stibnite and post-stibnite gold grains.

The pre-stibnite gold grains are wholly or

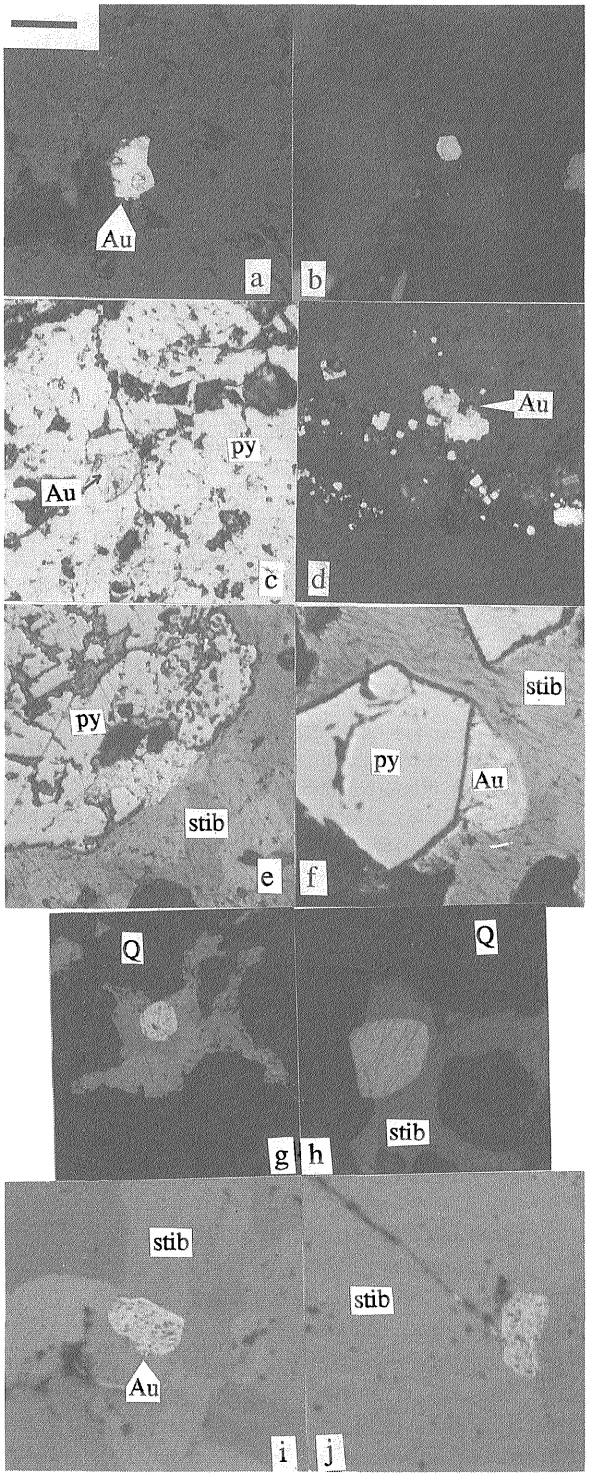

Fig. 8 Photomicrographs showing native gold occurrences at the Wuxi deposit. Scale bar=25 micrometers, reflected light. a, gold grain in quartz aggregation; b, a euhedral gold crystal (?) occurring in quartz crystal; c, gold filled in etched pits of coarse pyrite; d, gold grain occurring in fine grained pyrite band; e, gold filling in etched pits of pyrite and enveloped by stibnite; d, gold grain precipitated on pyrite surface included in a stibnite crystal; g, round gold grain enveloped in stibnite; h, round gold grain partly enveloped in stibnite crystal; i, gold occurring in crystal boundary of stibnite; j, gold grain included in stibnite crystal and filled in fissure of the crystal.

partly enveloped in stibnite crystals and exhibit rounded shapes ranging from several to about 100 micrometers (Figs. 8g and 8h). The gold filled etch pits of pyrite also predates stibnite because both pyrite and gold are included by stibnite (Fig. 8e). The syn-stibnite gold is indicated by micro-veins consisting of stibnite and native gold filled fissures in quartz (Figs. 9a, 9b and 10). The dendritic native gold occurs in the open space of the fissure. Gold grains filling in fissures are apparently larger than those included in pyrite, stibnite crystals or disseminated in quartz aggregates. Native gold fissures from the Wuxi deposit which can be observed by unaided eyes were found during the mining. Post-stibnite gold precipitation is indicated by intercrystal gold grains and/or gold grains filling in fissures within stibnite crystal (Figs. 8i and 8j).

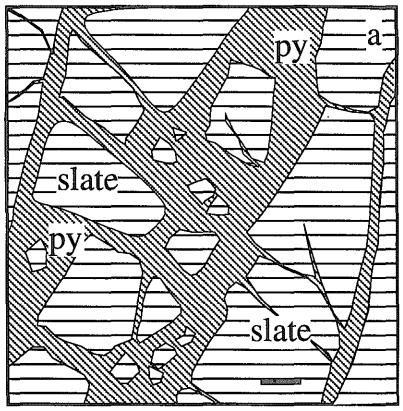

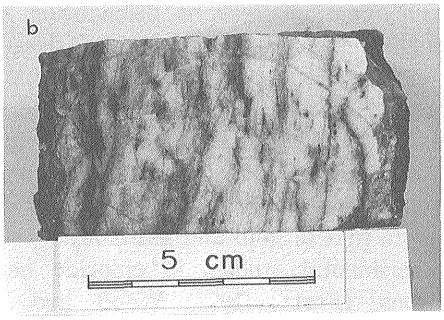

Fig. 9 a, Sketch of pyrite veinnet (py) in slate (S) (in host rock adjacent to No. 1 vein, west gallery of -60m level), scale bar=1cm; b, Photograph of banding quartz vein formed by pyrite filling in fissures of quartz vein.

In a euhedral quartz crystal of phase 6 (stibnite-quartz vein phase), a native gold grain exhibiting a hexoctahedral crossection typical of euhedral crystals with a diameter of about 12 micrometers (Fig. 8b) was observed.

Native gold occurrences mentioned above indicates that gold mineralization at the Wuxi deposit started at vein phase 5 and lasted until the end of the phase 6 and is later than the main vein phase (phase 4) consistent with geological evidence indicating that the gold ore body is controlled by secondary folds superimposed on composite quartz veins. In addition to a longer lasting period of gold precipitation than that of stibnite, gold and stibnite belong to products of the same mineralization stage.

Therefore, mineralization at the Wuxi deposit can be divided into two stages of tungsten mineralization stage (I) and gold-antimony mineralization stage (II). The former can be divided into two substages corresponding the formation of scheelite-quartz veins (substage Ia) and wolframite quartz veins (substage Ib). Gold and antimony mineralization are later than tungsten mineralization. Stage I corresponds to vein phases 2 and 3, stage II to vein phases 5 and 6.

5. Discussion

5.1 Deposit type

The recognition of deposit type highly depends on classification criteria adopted. For the purpose of exploration and prospecting, the Wuxi deposit was categorized as bedded type hosted in detrital rocks based on the classification of occurrence mode and comparison of various antimony mineralizations in China (Hu *et al.*, 1996). The Wuxi deposit was also referred to as a stratabound gold, tungsten or antimony deposit respectively (Liu *et al.*, 1983; Bao, 1988, 1990). However, what "stratabound deposit" means here is different from its original concept which is widely accepted. For example, tungsten mineralizations in Austria and West Greenland

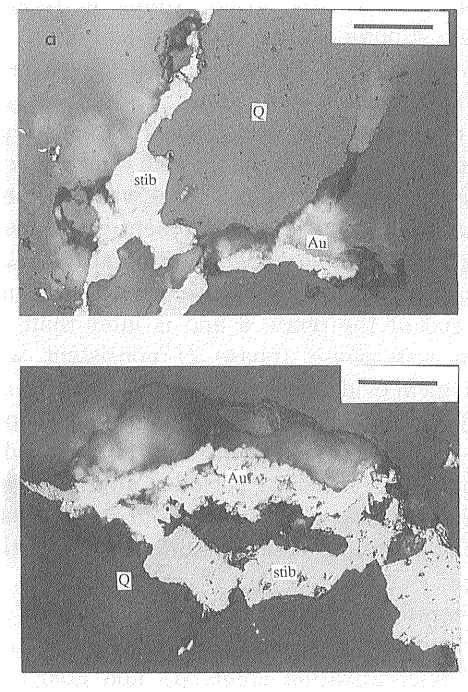

Fig. 10 Photomicrographs (a and b) showing native gold (light gray) and stibnite (gray) filled in fissures of quartz (black and dark gray) vein. Scale=50 micrometers.

are hosted in calc-silicate rocks which underwent amphibolite facies metamorphism, and scheelite mineralization formed prior to the main metamorphism (Raith, 1991; Appel, 1994). At Wuxi, the country rock surrounding the mineralization is lithologically homogeneous calcareous-slate, mineralization is strongly structurally controlled rather than lithologically controlled. Geological characteristics of the Wuxi deposit described earlier suggest it should categorized as a composite W-Au-Sb concordant bedding-parallel vein type mineralization. The vein type tungsten mineralization (stage Ia and Ib) and composite gold-antimony mineralization in fractured or brecciated bedding-parallel veins and country rocks are spatially coupled. A summary of the detailed deposit features is as follows:

1) Mineralization occurs in interlayer faults under a regional background of detachment structures;

2) Quartz veins are concordant with bedding horizons of the country rock, occurring as interlayer-fault filling and consisting multiple phases;

3) Tungsten mineralization is of vein type consisting of scheelite-bearing quartz veins and wolframite quartz veins;

4) Gold and antimony mineralizations are characterized by filling of fractured or brecciated bedded veins as well as slate and are later than tungsten mineralization and postdate the formation of the main quartz veins.

The Wuxi deposit is a representative spatially-coupled vein type tungsten mineralization, and fracture filling composite gold-antimony mineralization. Both of these are significant deposit types in the Xuefeng belt.

5.2 Hydrothermal history at the Wuxi deposit

The hydrothermal history at the Wuxi deposit was well recorded by composite quartz veins which resulted from periodic discharge of deep hydrothermal fluids. Hydrothermal discharge at Wuxi might have been structurally initiated and stimulated. Detachment faults (interlayer faults) as well as later brittle fractures in quartz veins in the Wuxi area served as dilation structures delivering open space for hydrothermal mineral deposition. Periodic structural mobilizations of interlayer detachment faults is indicated by the occurrence of multi-phase veins.

Various mineralizations at Wuxi indicates the chemical changes of discharging fluids through ore mineral paragenesis. Two mineralization stages responsible for tungsten mineralization (I) and gold-antimony mineralization (II) may have resulted from two kinds of hydrothermal fluids because transportation and deposition conditions of tungsten is different from that of gold and antimony.

Experimental studies in chloride bearing solutions (Forst, 1977; Wood and Vlassopoulos, 1989; Wood, 1992) indicate the chemical species H_2WO_4 (aq) is responsible for W transport in hydrothermal solutions according to:

$$WO_3 + H_2O(l) = H_2WO_4(aq) \quad (1)$$

Solubility of tungsten mineral as a simple oxyacid species can attain values between 10 to 100 ppm under geologically reasonable conditions without any complexation with additional ligands (Wood, 1992). Scheelite deposition can be expressed by the reaction:

$$H_2WO_4(aq) + Ca^{2+} = CaWO_4(scheelite) + H^+ \quad (2)$$

These reactions demonstrate that scheelite dissolution and W transport take place in acidic solution and scheelite precipitation is caused by increasing of pH value (neutralization of solution). Experimental data (Wood, 1992) (Fig. 11a) show a dramatic drop of W concentration with increases in pH value from 3 to 5. Such neutralization of fluids can arise from interaction with $CaCO_3$ in host rocks.

Tungsten solubility is also strongly affected by temperature. Scheelite solubility according to reaction (2) is prograde from 300 to 400°C, but is thereafter retrograde from 400 to 600°C (Wood, 1992). According to Wood (1992), scheelite precipitation takes place at a blocking temperature between 300 to 400°C during cooling of hydrothermal solutions. It is therefore proposed that hydrothermal solutions responsible for scheelite mineralization (phase 2) at the Wuxi deposit may have resulted from acidic aqueous fluids containing tungsten oxyacid and scheelite deposition most likely took place through cooling and interaction with calcareous slate.

The formation of ferberite-quartz veins indicates the existence of Fe^{2+} cation in solution because Mn/Fe ratio of "source material" is the most important factor controlling wolframite composition (Hsu, 1976). Chlorine complexes may be the possible species of iron in solution. Theoretical calculation demonstrates that wolframite can precipitate in acidic reduced solutions rich in calcium and iron (Zhang, 1989). According to the replacement reaction between wolframite and scheelite:

$$FeWO_4(wolframite) + CaCO_3 = CaWO_4(scheelite) + CO_2 + Fe^{2+} \quad (3)$$

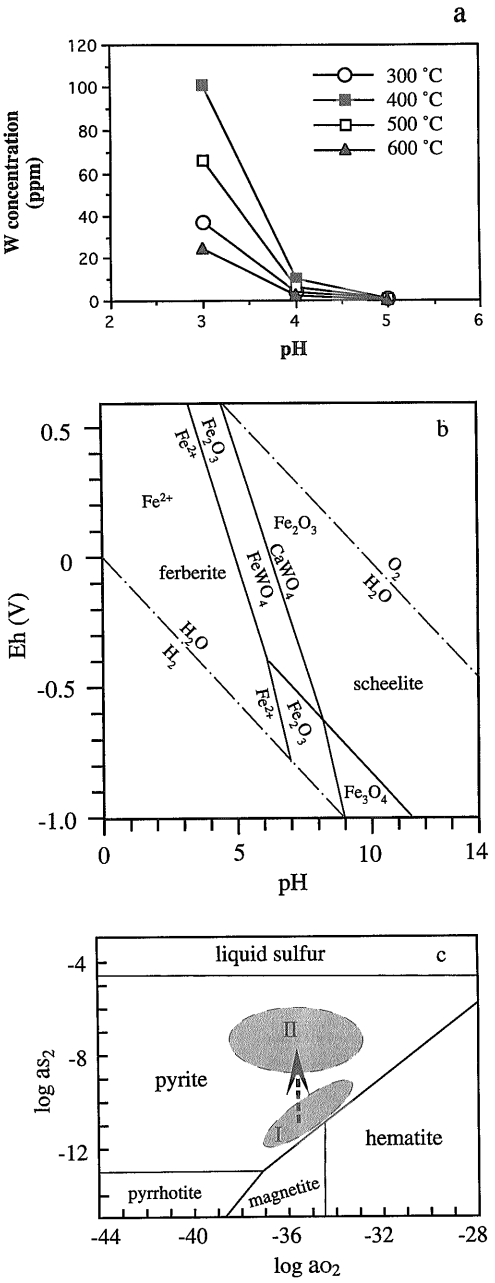

Fig. 11 a, Scheelite solubility vs. pH for reaction of $CaWO_4+2H^+=Ca^{2+}+H_2WO_4$ (aq); b, Eh-pH diagram showing stability fields of scheelite and ferberite in aqueous solution at 300°C (simplified after Schröcke at al., 1984); c, fs_2 vs. fo_2 diagram showing the possible condisions of mineralization stage I and the fs_2 increase from stage I to stage II.

Ferberite is stable under acidic and a high Pco_2 conditions which differs from the alkaline environment responsible for scheelite deposition. According to Schröcke *et al.* (1984), stability fields of scheelite and ferberite in Eh-pH diagrams of Fe-W-O-OH and Fe-Ca-W-O-OH systems are distinguished largely by pH value (Fig. 11b). Hsu's data (1976, 1977) demonstrate that scheelite and ferberite have similar wide stability fields of oxygen and sulfur fugacities, which range from adjacent magnetite/pyrrhotite-hematite/pyrite boundary in fo_2-fs_2 diagram to high fo_2 conditions. The paragenetic pyrite and lack of hematite at Wuxi place constraints on a narrow field below the hematite/pyrite boundary in fo_2-fs_2 diagram for formation of ferberite quartz veins (Fig. 11c).

Therefore, ferberite precipitation (phase 3) most likely resulted from decrease in pH (acidation of solution) in contrast to the neutralization process responsible for scheelite deposition. Such acidation seems unlikely to be the result of in situ fluid-rock interaction because the host rock is calcareous slate and ferberite-quartz veins appear as a later phase overprinting the scheelite-quartz phase. A probable explanation for acidation of ore-forming fluid is the chemical changes of the discharging solution originating from a deeper variety of parent solution, such as the increase of fluid fs_2 which is indicated by the occurrence of paragenetic pyrite.

Gold mineralization at the deposit started at pyrite-quartz phase (phase 5) which predates antimony mineralization. Within fine grained pyrite bands, rare stibnite can be observed which implies that the fluid responsible for this phase was too low in antimony concentration to precipitate abundant stibnite. However, gold and antimony mineralization are closely related to each other in the phase 6 which is clearly indicated by the paragenetic native gold and stibnite. The correlation coefficient between gold and antimony grades of No. 4 vein is 0.79, that of gold and antimony contents in altered slates is 0.67 (Liu *et al.*, 1983). Experimental studies of Wood *et al.* (1987), Krupp (1988), and Hu (1994) provide a comprehensive understanding of gold and stibnite solubility. According to these studies, thioantimonite complexes ($H_2Sb_2S_4^0$, $HSb_2S_4^-$, $Sb_2S_4^{2-}$), hydroxothioantimonite complex ($Sb_2S_2(OH)_2^0$ and/or hydroxy complex are the dominant chemical species of antimony in solutions. Gold and antimony have higher solubility in alkaline solutions than in acidic solution. High fs_2 solution is required for antimony transport. Gold can be co-transported as bisulfide complexes with hydroxy antimony complexes in chloride-free aqueous solution. Kolpakova and Manucharyants (1990) also proposed the existence of $H_2AuSb_3^0$and $HAuSbS_3^-$in solutions. Temperature and pH value are two significant factors controlling antimony and gold solubility by affecting chemical species in solution. Acidation and cooling are two important mechanisms causing stibnite and gold deposition. The acidation of solution which most likely resulted from decomplexation of antimony-, gold-bisulfide complexes was clearly recorded by etched scheelite cemented by later phase quartz and stibnite (Figs. 6a and 6b).

There were obvious changes of pH and fS_2 values of ore forming fluids between the scheelite and stibnite phases of mineralization. Based on the homogenization temperatures (Luo *et al.*, 1984; Liu *et al.*, 1991; Shi *et al.*, 1993) and mineral assemblege in various vein phases, we summarize a brief hydrothermal history of the Wuxi deposit in Figure 12. Hydrothermal temperature decreases from the earlier to later phases (Fig. 12a). Cooling was a fundamental hydrothermal process in Wuxi. The pH and log as_2 values of solutions increase from tungsten mineralization (stage I) to gold-antimony mineralization (stage II) (Figs. 11c, 12a and 12b) assuming no significant change in fo_2.

The chemical changes of the ore-forming fluids at Wuxi are also indicated by trace element contents of the ore-minerals. For example, the auriferous pyrite and stibnite are characterized by high arsenic concentrations. The As content of pyrite increases obviously from fresh slate (20ppm) to altered slate (2770 ppm) and to quartz veins (4600ppm) which is

consistent with the increase of gold content of pyrite from 2.5 to 81.2 and 73.7ppm (Bao and He, 1991). This demonstrates that ore-forming fluids responsible for Au-Sb mineralizations were enriched in arsenic concentrations. The geochemical association of arsenic and antimony in many hydrothermal deposits and geothermal waters is well known. Such association can be well understood based on the similar stable conditions of arsenic sulfide complexes and antimony sulfide complexes within the pH range of typical geochemical systems (Spycher and Reed, 1989). The preferential accumulation of visible gold on arsenic enriched pyrite was explained to be an electrochemically dominated process (Möller, 1993; Möller and Kersten, 1994). According to their studies, arsenic is the most important element

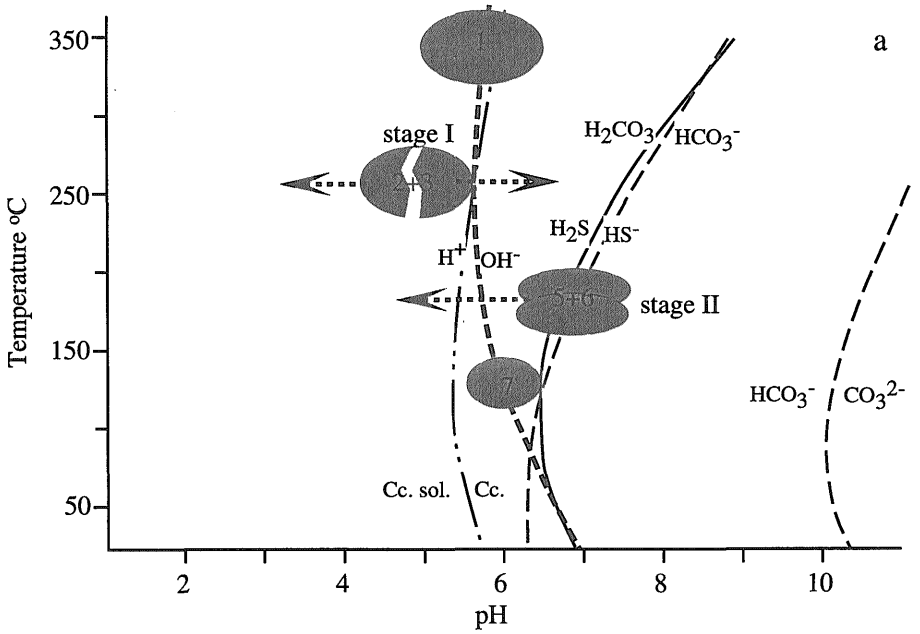

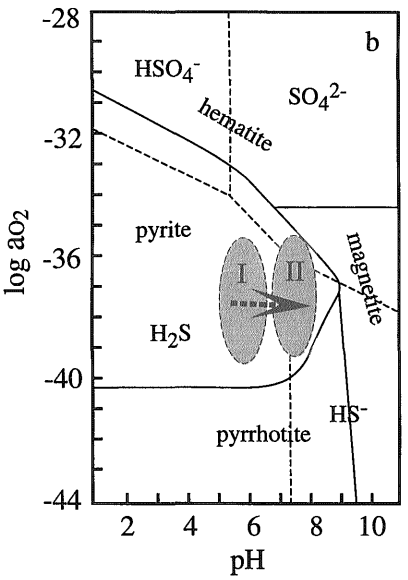

Fig. 12 a, A brief hydrothermal history responsible for various phases of composite quartz vein (from pre-ore phase (1) through scheelite phase (2), wolframite phase (3), pyrite phase (5), stibnite phase (6) to post-ore phase (7). The arrows represent chemical processes (acidation and neutralization) resulting in ore mineral precipitation. The curves represent equal activities of aqueous and separate their regions of predominance. Cc=calcite, (After Barnes, 1979, Fig. 8.5); b, possible pH increase of ore-forming fluid from tungsten mineralization stage (I) to gold-antimony mineralization stage (II) shown in the fo_2 vs. pH diagram at 250°C (After Barnes, 1979).

in establishing p-type conductivity of pyrite and arsenopyrite, and Au accumulates at p-type conductors in n-p junctions.

5.3 Modeling of Au, Sb and W mineralization at Wuxi related to geological evolution

Geological constraints on the timing of geological evolution and tungsten, gold and antimony mineralization are given in Table 1 and demonstrate that the Mesozoic Era is an important period for development of ore-controlling structures. Mineralization may have taken place in the Jurassic period, under a detachment structure background corresponding to the regional extensional environment of the Yanshanian period (Sun *et al.*, 1991). Periodic development of bedding-parallel fractures (interlayer faults) as well as overprinting of sliding folds are important elements of the structural model for the formation of composite bedding-parallel quartz veins and composite mineralization.

Timing of mineralization does not support metamorphic models (Liu *et al.*, 1983; Luo *et al.*, 1984) which assume that mineralization took place during the Xuefengian or Caledonian periods. Lack of spatial relationships between mineralization and magmatic intrusion in the mining area, even in a larger scale area, makes it difficult to develop the hypothesis of magma devolatilization. Compared with tungsten deposits and antimony-tungsten deposits related to magmatic activity (Chen *et al.*, 1985; Chen and Sun, 1987; Shi and Hu, 1988), the composition of wolframite and antimony mineral association at the Wuxi deposit do not support the model of fluid origin from magmatic intrusion.

The results of our research suggest a model for the origin of hydrothermal fluids involving deep convection and chemical evolution of paleo-ground water (Shi *et al.*, 1993; Shi and Hu, 1994). The penetration of water through rock units in the brittle regime of the continental crust can extend to 12-15km estimated on the basis of the brittle-ductile transition at temperatures of 350 to 450°C (Nesbitt and Muehlenbachs, 1988). Fluid inclusion studies (Luo *et al.*, 1984; Shi *et al.*, 1993) indicate that fluids responsible for the composite quartz veins in Wuxi are low salinity aqueous solutions. In contrast to the genetic model for Hg, Sb and mesothermal Au deposits of the Canadian Cordillera (Nesbitt and Muehlenbachs, 1988), we emphasize that paleo-ground water may play a more important role than meteoric water during the circulation of fluids based on considerations of paleohydrology and mineralization timing, even though the fluid was mostly likely a mixture of many kinds of free water in rock units including paleo-ground water (fossil water) and meteoric water as well as others. The fluid chemistry evolves through fluid-water interactions and varies from different circulation systems.

The Middle to Upper Proterozoic unit is characterized by high gold, tungsten and antimony concentrations and has been emphasized to be the source of gold, tungsten and antimony (Liu *et al.*, 1983; Luo, 1990). The average gold concentration of pre-Cambrain systems varies from 6.5 to 14.0ppb (Liu *et al.*, 1983) or from 1.8 to 9.0ppb (Luo, 1990). Tungsten and antimony exhibit a similar preliminary enrichment in the Proterozoic rocks, especially in the volcanic rocks. It is possible that the basement rock in Hunan serves as the ultimate source of mineralizations and is of no importance as a protore. An antimony enriched geochemical block mainly composed of the Middle to Upper Proterozoic unit and the Lower Paleozoic group has been proposed to be responsible for the high antimony mineralization in Hunan (Hu, 1995). The convecting fluids aquire Si, W, Au, Sb and S which were precipiated later at Wuxi through interaction with the Proterozoic rocks.

The deep convection system of fluids is likely initiated or promoted by structural deformation, especially the development of brittle faults or the change of fault property from ductile to brittle. The brittle fracture zone will connect various underground water systems and allows for water discharge from one system to another. Such discharge is mainly controlled by fluid pressure difference between two systems.

The downward-migrating water will be

exposed to a larger rock surface area producing lower water/rock ratio and the rocks will impose their chemical characteristics on the fluids that flow through them by interactions. In shallow circulation systems characterized by high water/rock ratios, the fluids retain geochimical characteristics that most closely resemble those of the parent fluids. With respect to low water/rock ratio circulation systems at deeper levels, the fluids acquire geochemical characteristics that resemble those of the controlling lithologies. A fluid that closely resembles a fluid produced by metamorphic devolatilization will be the end result of downward-migrating process (Nesbitt and Muehlenbachs, 1988). The water/rock ratio estimated on oxygen isotope data also implies the possible depth of circulation system and the geochemical characteristics of the fluids.

Mineralization may mainly relate to upward discharge processes of deeper fluids which accompany multiple physical-chemical changes resulting in precipitation of hydrothermal minerals, e.g., cooling, depressurization, mixture of different fluids as well as change in redox state. Hydrothermal minerals record more evidence of discharge process rather than pre-influx history. The ore-forming fluids in the Wuxi deposit were characterized by high and variable $\delta^{18}O$ values. Various vein phases exhibit an obvious decrease of $\delta^{18}O$ value from stage 1 (13.6%) through phase 2+3 (8.0-9.8%), phase 5+6 (4.3-7.2%) to phase 7 (2.0%) (Luo *et al.*, 1984). However, the mixture model of metamorphic fluid with meterioc water proposed by Luo *et al.* (1984) cannot account for the remarkable chemical changes of ore-forming fluids which we discussed earlier. According to our model, fluids which circulated in different environments with variable water/rock ratios must have been involved in the formation of composite quartz veins. At the beginning of hydrothermal activity, deeper solutions with higher temperatures and geochemical characteristics consistent with flow in low water/rock ratio systems were discharged at the deposit site with little mixture with shallow water. Then shallower hydrothermal fluids with lower temperatures were allowed to discharge or shallower fluids were added to the deeper discharging fluids. In the final stage, the discharging fluids were mainly composed of solutions characterized by low temperatures and characteristics typical of flow through high water/rock ratio systems. Tungsten-bearing fluids may have originated from deeper systems and gold-antimony bearing fluids represent relatively shallower hydrothermal systems.

6. Conclusions

It has been shown that the Wuxi deposit can be categorized as a bedding-parallel vein type composite tungsten, gold-antimony mineralization. Mineral associations of scheelite, wolframite, native gold and stibnite are hosted by Proterozoic slate and controlled by detachment structures. Based on our re-examination of the geology and mineralization, the following can be concluded (proposed):

1) Mineralization took place during the Jurassic under a structure background of detachment faulting;

2) Periodic dilation of bedding-parallel fractures is responsible for formation of composite quartz veins and composite mineralizations. Quartz veins can be divided into seven phases and mineralization is divided into two stages;

3) Tungsten mineralization and gold-antimony mineralization resulted from two kinds of fluids which are low salinity aqueous solutions with variable chemical properties and temperatures. Neutralization and acidation of solutions are possible mechanisms for scheelite deposition and ferberite precipitation, respectively. Gold and antimony share a similar origin and were probably transported by the same reduced solution characterized by high fs_2. Cooling and acidation might be the significant mechanisms for stibnite and gold precipitation. There are obvious changes in pH and fs_2 values of the ore-forming fluids between scheelite deposition and gold-antimony mineralization. The deposit is thus categorized as a spatially coupled tungsten mineralization and

gold-antimony mineralization;

4) The Wuxi deposit can be genetically interpreted according to a model for the origin of fluid involving deep convection, chemical evolution and discharge of paleo-ground water. Brittle faulting would connect a deeper hot fluid system and allow for discharge to a shallower system. The mineralization most likely takes place at the discharge location. Periodic structural activity allowed spatial coupling of tungsten and gold-antimony mineralization at the Wuxi deposit.

Acknowledgments: This paper was finished during X. H.'s stay at the Geological Survey of Japan which was financially supported by the Science and Technology Agency (STA) of Japan Fellowship. The authors would like to express their sincere thanks to Prof. M.K. Shi at the Yichang Institute of Geology and Mineral Resources, Chinese Academy of Geological Science, for beneficial discussion, to Mrsses Z.L. Zou, L.J. Luo and Y.H. Gao at the Xiangxi Gold Mine, Hunan, China, for their assistance in the field. We are grateful to Dr. C.W. Mandeville for helpful comments and English corrections to an earlier version of this manuscript.

References

Appel, P.W.U. (1994) Stratabound scheelite in altered Archaean komatiites, West Greenland, *Mineral. Deposita*, **29**, 341-352.

Aral, H. (1989) Antimony mineralization in the northern Murat Dagi (western Turkey). *Economic Geology*, **84**, 780-787.

Bao, Z. (1990) Geological features and exploration guides of the W-Sb-Au deposits in western Hunan Province. *Geology and Prospecting*, no. 2, 17-23 (in Chinese with English abstract).

Bao, Z. and He, G. (1991) Geologic and geochemical features of Wuxi W-Sb-Au ore deposit in western Hunan. *Hunan Geology*, **10**, no. 3, 207-216 (in Chinese with English abstract).

Bao. Z. (1988) Occurrence features, metallogenesis and exploration guide of a stratabound scheelite deposit in western Hunan. *Geology and Prospecting*, no. 3, 15-20 (in Chinese with English abstract).

Barnes, H.L. (1979) Solubilities of ore minerals. *In* H.L. Barnes, eds., *Geochemistry of Hydrothermal Ore Deposits*, 404-460.

Chen, D. and Sun, S. (1987) Metallic minerals and mineral assemblage of the Chashan antimony-polymetallic deposit in Guangxi. *Bulletin of the Institute of Mineral Deposits, Chinese Academy of Geological Sciences*, no. 1, 89-97 (in Chinese with English abstract).

Chen, D., Lu, J., Sun, S., Lin, Y. and Chen, K. (1985) A preliminary study on berthierite, Chashan, Guangxi. *Acta Mineralogica Sinica*, **5**, no. 3, 208-215 (in Chinese with English abstract).

Dill, H. (1985) Antimoniferous mineralization from the Mid-European Saxothuringian zone: mineralogy, geology, geochemistry and ensialic origin. *Geologische Rundschau*, **74/3**, 447-466.

Dill, H.G., Weiser, T., Bernhardt, I.R. and Kilibarda, C.R. (1995) The composite gold-antimony vein deposit at Kharma (Bolivia). *Economic Geology*, **90**, 51-66.

Foster, R.,P. (1977) Solubility of scheelite in hydrothermal chloride solutions. *Chemical Geology*, 20, 27-43.

Guillemette, N. and Williams-Jones, A.,E. (1993) Genesis of the Sb-W-Au deposits at Ixtahuacan, Guatemala: evidence from fluid inclusions and stable isotopes. *Mineral Deposita*, **28**, 167-180.

Gumiel, P. and Arribas, A. (1987) Antimony deposits in the Iberian peninsula. *Economic Geology*, **82**, 1453-1463.

Hsu, L.,C. (1976) The stability relations of the wolframite series. *American Mineralogist*, **61**, 944-955.

Hsu, L.,C. (1977) Effects of oxygen and sulfur fugacities on the scheelite-tungstenite and powellite-molybedenite stability relations. *Economic Geology*, **72**, 664-670.

Hu, X. (1994) Characteristics and discussion of stibnite solubility in different solutions. *Bull. Yichang Inst. Geol. Min. Res., CAGS*, no. 20, 32-42 (in Chinese with English abstract).

Hu, X. (1995) The geological setting and genesis of Xikuangshan super-giant antimony deposit, Hunan, China. Unpublished Ph. D. thesis, Graduate School of Chinese Academy of Geological Sciences, 173 p. (in Chinese with English abstract).

Hu, X., Murao, S., Shi, M. and Li, B. (1996)

Classification and distribution of antimony deposit in China. *Resource Geology* **46**, 287-297.

Hunan Bureau of Geology and Mineral Resources (1988) Regional Geology of Hunan Province. People's Republic of China, Ministry of Geology and Mineral Resources, Geological Memoirs, series 1, number 8, Geological Publishing House, Beijing, 718 p. (in Chinese with English abstract).

Kolpakova, N. N. and Manucharyants, B. O. (1990) Physical-chemical conditions of formation of stibium and gold-stibium mineralization. *Geokhimia*, no. 12, 1756-1766 (in Russian).

Krupp, R.,E. (1988) Solubility of stibnite in hydrogen sulfide solutions, speciation, and equilibrium constants, from 25 to 350°C. *Geochimica et Cosmochimica Acta*, **52**, 3005-3015.

Li, J. (1989) Geological features of the Woxi Au-Sb-W ore deposit. *Geology and Prospecting*, **25**, no. 12, 1-7 (in Chinese with English abstract).

Li, T. (1987) Xuefengshan Au-Sb-W ore belt in Hunan Province: the metallogenic regularity and minerogenesis of its west segment. *Geology and Prospecting*, **23**, no. 11, 1-5 (in Chinese with English abstract).

Liang, B. and Zhang Z. (1986) A study on the typomorphic properties of quartz in Woxi Au-Sb-W deposit, western Hunan. *Hunan Geology*, **5**, no. 2, 17-25 (in Chinese with English abstract).

Liu, J. (1993) Genetic model for gold deposits in the Xuefeng geodome. *Geotectonica et Metallogenia*, **17**, 127-134 (in Chinese with English abstract).

Liu, R. (1992) Detachment structure in coal area, Hunan Province. *Hunan Coal Geology and Exploration*, no. 1 (in Chinese).

Liu, Y. (1993) Study of dynamic mineralization of fracture structure in Woxi gold deposit, Hunan Province. *Journal of Chendu College of Geology*, **20**, no. 1, 50-55 (in Chinese with English abstract).

Liu, Y., Zhang J., Qiao, E., Mao, H. and Zhao, M. (1983) Geochemistry of gold deposits in west Hunan and east Guangxi, China. *Geochimica*, no. 3, 227-240 (in Chinese with English abstract).

Luo, X. (1990) On the source of ore-forming substances of pre-Cambrian gold deposits in Hunan Province, *Journal of Guilin College of Geology*, **10**, no. 1, 13-26 (in Chinese with English abstract).

Luo, X., Yi, S. and Liang, J. (1984) On the genesis of the Wuxi gold, antimony and tungsten deposit, western Hunan. *Journal of Guilin College of Geology*, no. 1, 21-35 (in Chinese).

Möller, P. (1993) Why is gold accumulated in pyrite- and arsenopyrite-rich mineralizations? An electrochemical approach. *In* Fenoll Hach-Aclí, Torres-Ruiz and Gervilla, eds., *Current Research in Geology Applied to Ore Deposits*, 503-506.

Möller, P. and Fersten, G. (1994) Electrochemical accumulation of visible gold on pyrite and arsenopyrite surfaces. *Mineral. Deposita*, **29**, 404-413.

Nesbitt, B.E. and Muehlenbachs, K. (1988) Geology, geochemistry, and genesis of mesothermal lode gold deposits of the Canadian Cordillera: Evidence for ore formation from evolved meteoric water. *Economic Geology Monograph* 6, 609-628.

Peng, B. (1991) A preliminary study on the tectonogeochemistry of the Woxi fault, western Hunan, China. *Geotectonica et Metallogenia*, **15**, 118-127 (in Chinese with English abstract).

Raith, J.G. (1991) Stratabound tungsten mineralization in regional metamorphic calc-silicate rocks from the Austroapline Crystalline Complex, Austria. *Mineral. Deposita*, **26**, 72-81.

Schröcke, H., Trumm, A. and Hochleitner, R. (1984) Über den Transport von wolfram und den Absat2 von Wolfram-Doppel-Oxiden in fluiden wässrigen Lösungen. *Geochimica et Cosmochimica Acta*, **48**, 1791-1805.

Shao, J., Wang, P. and Chen D. (1989) Characteristics of mineralized alteration zone in Woxi Au-Sb-W deposit, western Hunan. *Hunan Geology*, 8, no. 2, 39-48 (in Chinese with English abstract).

Shi, M. and Hu, X. (1988) The geological characteristics and genesis of the granite-hosted tungsten deposit at Dajishan mine, Jiangxi province, China. *In*, *Proceedings of the Seventh Quadrennial IAGOD Symposium*, 613-621.

Shi, M. and Hu, X. (1994) Antimony mineralization in paleo-hydrothermal-active field. the 9th IAGOD Symposium, Beijing (abstract).

Shi, M., Fu, B., Jin, X. and Zhou, X. (1993) Antimony metallogeny in the central part

of Hunan Province, China. Hunan Press of Science and Technology, Changsha, 151 p. (in Chinese with English abstract).

Spycher, N. and Reed, M.H. (1989) As (III) and Sb (III) sulfide complexes: An evaluatin of stoichiometry and stability from existing experimental data. *Geochimica et Cosmochimica Acta*, **53**, 2185-2194.

Sun, Y., Shen, X., Shu, L. and Shi, Z. (1991) On evolution of the time-order structures of compressive orogeny and extensional basin formation in north Jiangxi and Hunan Provinces. *Geotectonica et Metallogenia*, **15**, 160-169 (in Chinese with English abstract).

Wang, F. and Yang, R. (1990) The geologic feature of the stockwork veinlet orebody in Woxi gold-antimony-tungsten deposit, Yuangling County. *Hunan Geology*, **9**, no. 1, 52-53 (in Chinese with English abstract).

Wang, J. (1986) Geochemical studies of the Xi'an tungsten ore deposit, west Hunan, China. *Geochimica*, no. 2, 183-192 (in Chinese with English abstract).

Wang, X. (1993) Study on mineralogic characteristics of quartz from Xiangxi Gold Mine. *Mineral Resources and Geology*, **7**, no. 4, 278-281 (in Chinese).

Wood, S,A. (1992) Experimental determination of the solubility of WO_3(s) and the thermodynamic properties of H_2WO_4(aq) in the range 300-600°C at 1 kbar: calculation of scheelite solubility. *Geochimica et Cosmochimica Acta*, **56**, 1827-1836.

Wood, S.,A, Crerar, D.,A. and Borcsik, M.,P. (1987) Solubility of the assemblage pyrite-pyrrhotite-magnetite-sphalerite-galena-gold-stibnite-bismuthinite-argentite-molybdenite in H_2O-NaCl-CO_2 solutions from 200-350°C. *Economic Geology*, **82**, 1864-1887.

Wood, S.A. and Vlassopoulos, D. (1989) Experimental determination of the hydrothermal solubility and speciation of tungsten at 500° C and 1 Kbar. *Geochimica et Cosmochimica Acta*, **53**, 303-312.

Wu, J., Xiao, Q. and Zhao, S. (1989) Antimony deposits of China. *In* S. Song, eds., *China Deposits*, volume 1, Geological Publishing House, Beijing, 209-287.

Xiao, Q. and Li, D. (1984) An investigation into the genesis of the antimony deposits in Hunan. *Mineral Deposits*, **3**, no. 3, 13-25 (in Chinese with English abstract).

Yang, S. (1986) On inquiry about the genesis of Hunan stibnite ore and the direction of ore search. *Hunan Geology*, **5**, no. 4, 12-25 (in Chinese with English abstract).

Zhang, L. (1985) Stable isotopic geology on the tungsten, antimony and gold deposits in Xuefengshan uplifted area, western Hunan. *Geology and Prospecting*, **21**, no. 11, 24-28 (in Chinese with English abstract).

Zhang, Y. (1989) The formation conditions of wolframite in the calcium-rich environment. *Mineral Deposits*, 8, no. 1, 65-69 (in Chinese with English abstract).

Au-Sb-W鉱化作用の成因モデル：中国湖南省沃溪鉱床の地質と鉱化作用に基づく考察

胡　雄偉・村尾　智・黄　緒烂

要　旨

湖南省西部の雪峰弧形隆起帯内に位置する沃溪鉱床は中国を代表するAu-Sb-W鉱床である．沃溪は欧州や南米のAu-Sb-W鉱床とは異なり地層面にほぼ平行な鉱脈群からなる．鉱脈の規模は走行方向に6 km，傾斜方向に1 kmで平均品位はAu8.38ppm，Sb4.36%，$WO_3$0.37%である．

鉱床の母岩はセリサイトを含み，紫がかった赤色を特徴とする石灰質頁岩で，板溪層群（中国での表記は板溪群）に属する．鉱体の位置は地層面にほぼ平行な断層と東北方向に伸びる2次褶曲に規制される．断層はデコルマンの特徴を示す沃溪断層に低角で接する．2次褶曲は中生代に形成されたものである．全体として鉱床はデタッチメント断層に強く規制されている．

鉱化作用は中生代に起きており，断層の周期的な広がりによる熱水の周期的供給を示す石英の複合脈

を特徴とする．複合脈のマクロストラクチャーから断層の運動は7回起こったと判断される．鉱化作用は断層運動の2，3，5，6期に起きており，タングステンの時期は2，3期，金とアンチモニーは，5，6期に対応する．ここでは鉱化作用に注目する視点から，タングステンの沈殿した時期をステージIと呼び，更に灰重石のIa期と鉄マンガン重石のIb期に細分する．金-アンチモニー鉱化作用の方は5期の黄鉄鉱-石英層と6期の輝安鉱-石英層からなるがこれをステージIIと呼ぶ．タングステンは恐らく酸性溶液に起因し，中和によって灰重石が，pH減少によってフェルベライトが沈殿したと考えられる．金とアンチモニーはややアルカリ性の溶液によって同時に運搬され冷却とpH低下で沈殿したと思われる．すなわち本鉱床はタングステン鉱化作用と金-アンチモニー鉱化作用という質的に異なるもの同士が空間的に接した結果と考えられる．

筆者らの研究によると沃溪の流体は地下深部で循環していた古地下水が化学的に進化したものである．鉱化作用の重要なメカニズムは深部から浅所への熱水の排出である．本地域に形成された断裂がその通路である．湖南においては中生代の断裂は周期的に活動しているが，その周期性が沃溪地区の複合脈形成の主因である．

（受付：1996年7月23日；受理：1996年10月28日）

中英対照表

Banxi Group	板溪群
Changsha	長沙
Fuzhuxi	符竹溪
Hunan	湖南
Mayidi Formation	馬底驿組
Mobin	漠滨
Wuxi	沃溪
Xi'an	西安
Xichong	西冲
Xuefeng arcuate uplifted belt	雪峰弧形隆起帯
Zhazixi	渣滓溪